Kinetic Study of Ethyl Octyl Ether Formation from Ethanol and 1-Octanol on Amberlyst 70

Jordi Guilera, Roger Bringué, Eliana Ramírez, Carles Fité, and Javier Tejero
Chemical Engineering Dept., Faculty of Chemistry, University of Barcelona, C/Martí i Franquès 1, 08028 Barcelona, Spain

DOI 10.1002/aic.14497
Published online May 22, 2014 in Wiley Online Library (wileyonlinelibrary.com)

An option to introduce bioethanol to diesel, improving at the same time its fuel quality, is by adding ethyl octyl ether (EOE). It can be obtained successfully by the dehydration reaction between ethanol and 1-octanol over acidic ion-exchange resins. In the present work, the kinetic study of EOE synthesis on Amberlyst 70 in the liquid phase is performed in a 20-cm^3 fixed-bed reactor and in a 100-cm^3 batch reactor at 423–463 K and 2.5 MPa. EOE synthesis takes place together with diethyl ether (DEE) formation as main side reaction. A mechanistic kinetic model in terms of component activities is proposed for EOE synthesis (E_a=105 ± 4 kJ/mol) and for DEE formation (E_a =100 ± 5 kJ/mol). Reaction rates were highly inhibited by the adsorption of the formed water on Amberlyst 70. The inhibitor effect of water is well represented as a competitive adsorption with alcohols reactants on the catalysts surface. © 2014 American Institute of Chemical Engineers *AIChE J*, 60: 2918–2928, 2014
Keywords: ethyl octyl ether, diethyl ether, Amberlyst 70, kinetics, modeling

Introduction

Linear ethers with at least nine carbon atoms show high cetane numbers and desirable cold flow properties as light diesel fuel components.[1–3] Additionally, the use of alcohols coming from renewable sources to form such ethers is a chance to increase the biofuel percentage into the diesel pool. A compound that fulfills both requirements is ethyl octyl ether (EOE) with 10 carbon atoms, 10 w/w % oxygen content, boiling point of 460 K, density of 771 kg/m^3, cetane number of 97, and satisfactory lubricity.[1,4]

EOE can be synthesized in only one reaction step from the dehydration reaction between ethanol (EtOH) and 1-octanol (OcOH).[4–6] As Figure 1 illustrates, the desired reaction between the two alcohols to obtain EOE takes place in parallel with the intermolecular dehydration of two OcOH molecules to form di-*n*-octyl ether and that of two EtOH molecules to form diethyl ether (DEE). From an industrial standpoint, the differences between EOE, di-*n*-octyl ether, and DEE as possible candidates for diesel blends are relevant. DEE has a potential interest as a diesel compound because it is completely produced from bioethanol. In addition, the cetane number of DEE is really high (∼90) in comparison to that of EtOH (∼8), or that of commercial diesel fuel (40–55).[1,4] However, the high volatility of DEE is a serious drawback for its addition in large quantities to diesel blends. Conversely, EOE and di-*n*-octyl ether are linear long-chain ethers with excellent properties as diesel components.[5]

EOE can be successfully synthesized using acidic ion-exchange resins as catalysts.[4–6] The etherification reactions proceed smoothly from the beginning; being EOE and DEE formed in similar amounts and di-*n*-octyl ether in much lower ones. Accordingly, the main industrial drawback of EOE production is the loss of substantial amounts of EtOH to form DEE. In medium- and high-crosslinked macroreticular acidic ion-exchange resins such as Amberlyst 15, 16, 35, or 36, OcOH permeation is hindered whereas EtOH reach most of acid sites. As a result, DEE is preferably formed in such poorly swollen resins (selectivity to EOE 15–20% and to DEE 15–83%, with respect to EtOH). However, low-crosslinked resins such as Amberlyst 121, Amberlyst 70, or Purolite CT224 show wide enough spaces between polymer chains to allow OcOH access more easily to acid centers, and in this way, to compete efficiently with EtOH for the acid sites. Therefore, low-crosslinked resins maximized the production of EOE and reduced the amount of DEE formed (selectivity to EOE 41–46% and to DEE 43–53%, with respect to EtOH).[5]

Among low-crosslinked resins, the chlorinated Amberlyst 70 presents negligible desulfonation on EOE formation at temperatures as high as 463 K, whereas the thermal stability of common ion-exchange resins is limited to 393–423 K.[7–11] As a consequence, the use of Amberlyst 70 has been checked in reactions as esterification, etherification, oligomerization, acetalization, and Biginelli.[12–17] A much less reported commercial thermally stable resin is Purolite CT482. Such catalyst displays much higher acid capacity (4.25 mol H^+/kg) than Amberlyst 70 (2.65 mol H^+/kg).

Additional Supporting Information may be found in the online version of this article.

Correspondence concerning this article should be addressed to J. Tejero at jtejero@ub.edu.

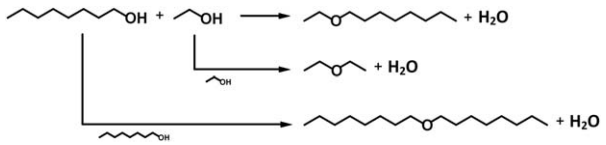

Figure 1. Reaction scheme of EOE production from 1-octanol and ethanol.[4]

Both catalysts recover completely their activity to EOE formation after drying, at least during 144 h. However, Purolite CT482 has a stiffer morphology in comparison to Amberlyst 70, by favoring the production of the less sterically demanding ether, DEE.[9] Therefore, Amberlyst 70 was chosen as the best acidic ion-exchange resin catalyst to produce EOE at relatively high temperature range (up to 463 K).

Alcohol dehydration, or else, alcohol acetalization reactions are well represented by Langmuir–Hinshelwood–Hougen–Watson (LHHW) or Eley–Rideal (ER) mechanisms.[18–27] LHHW mechanisms involve the reaction between an OcOH and an EtOH molecules adsorbed onto the resin; whereas in ER mechanisms, an alcohol molecule reacts from the liquid phase with a second alcohol molecule adsorbed onto the resin. To the best of our knowledge, the kinetics of EOE formation has not been determined, which is necessary for reactor modeling purposes. As for the formation of main side product, DEE, Kiviranta-Pääkkönen et al.[20] proposed an ER mechanism where an EtOH molecule is adsorbed and the second EtOH molecule reacts from the liquid phase.

In this work, the kinetic study of the reaction for obtaining EOE by the dehydration reaction between EtOH and OcOH on Amberlyst 70 in the liquid phase at the temperature range of 423–463 K was carried out to find a kinetic model that was able to predict reaction rates of EOE formation in a wide range of alcohol, ether, and water concentrations. Besides, a kinetic model for DEE formation is also proposed.

Experimental

Materials

OcOH (≥99 w/w %, Acros), EtOH (≥99.8 w/w %, Panreac), and DEE (≥99w/w %, Panreac) were used without further purification. EOE was produced and purified in our lab by rectification to ≥99 w/w %. Bidistilled water and N_2 (≥99.995 w/w %, Abelló Linde) were also used. Silicon carbide (SiC, Alfa Aesar) particles were used to dilute the resin catalyst. 1-Octene and di-*n*-octyl ether (≥97%, Fluka) were used for analysis purposes.

Catalyst

The acidic macroreticular polystyrene-codivinylbenzene resin Amberlyst 70 (Rohm and Haas) was used as catalyst. This commercial ion-exchange resin results from the macroreticular ion-exchange resin Amberlyst 39^{TM}. Some hydrogen atoms of benzene rings are replaced by chlorine by the action of a gas stream of chlorine. As a result, leaching of sulfonic groups are minimized up to temperatures as high as 463 K (preparation method patented by Rohm and Haas Company).[21] Its main properties are shown in Table 1. As seen, porosity of Amberlyst 70 appears in water or alcohol environment, while the resin is almost collapsed in dry state. In swollen state, Amberlyst 70 has a greatly expanded gel phase, comparable to low-crosslinked gel-type resins like Dowex 50Wx2.[9]

Table 1. Characteristics of Commercial Amberlyst 70[9]

Catalyst	Amberlyst 70
Structure	Macroreticular
Divinylbenzene (%)	7
Chlorinated	Yes
Skeletal density (kg/m^3)	1514
Acidity (mol H^+/kg)	2.65
T_{max} (K)	463
In Dry State	
Mean particle diameter, d_p (mm)	0.55
Surface area (m^2/g)[a]	0.02
In Water Swollen State	
d_p (mm)	0.86
Surface area (m^2/g)[b]	176
Volume of the swollen polymer phase, V_{sp} (m^3/kg)[b]	0.0014
Main polymer fraction density (nm^{-2})	0.4
In Alcohol Swollen State[c]	
d_p (mm)[d]	0.84

[a]BET method.
[b]Inverse steric exclusion chromatography technique.
[c]Laser diffraction technique.
[d]Mixture of OcOH and EtOH ($R_{OcOH/EtOH} = 10$).

Apparatus, analysis, and procedure

Experiments were performed in temperature range 423–463 K using two different reaction setups. A fixed-bed reactor was used to check the influence of OcOH, EtOH as well as EOE and DEE concentrations on the reaction rate. Besides the ethers, stoichiometric amounts of water are formed in the dehydration reaction of EtOH and OcOH. The effect of water concentration on the reaction rates was explored in the batch reactor.

Fixed-Bed Reactor. The setup consisted of a 20-cm^3 continuous fixed-bed reactor (PID Eng & Tech), schematically shown in Figure 2. The pressure was set at 2.5 MPa by means of a micrometric regulating valve, to assure that the reaction medium was in the liquid phase. The catalytic bed consisted of Amberlyst 70 homogeneously diluted with inert SiC particles. SiC was used to keep the bed isothermal, and also to assure good contact between the reaction medium and catalyst avoiding back-mixing and channeling. The catalytic bed was formed by catalyst ($d_p = 0.49 \pm 0.05$ mm) and inert ($d_p = 0.48 \pm 0.17$ mm) particles of similar size, as seen

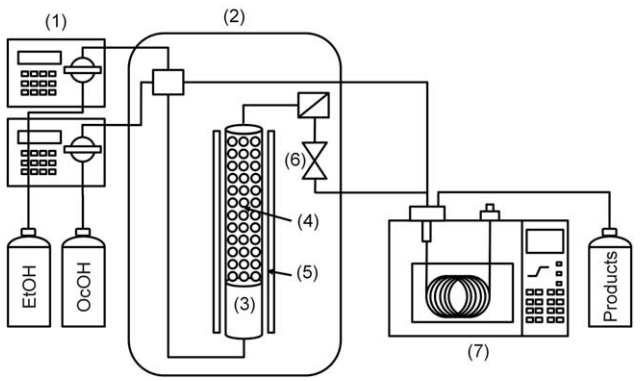

Figure 2. Scheme of the experimental setup.

(1) HPLC pumps, (2) hot box, (3) reactor, (4) catalytic bed, (5) electrical furnace, (6) regulating valve, and (7) GLC.

in Supporting Information Figure S1. The temperature was controlled within ±1 K by an electrical furnace. Liquid samples were taken in-line from the reactor inlet and outlet and injected directly into a GLC apparatus (HP6890A GLC, Hewlett Packard). Analysis procedure is described in detail elsewhere.[9]

Amberlyst 70 was dried in an atmospheric oven at 383 K overnight, prior to place it into the reactor. The water content of Amberlyst 70, determined by means of an Orion AF8 Karl Fisher titrator, was ≤2.25 w/w %. Then, dried catalyst samples (0.1–2 g) were diluted in inert SiC (12–15 g). After filling the reactor and placing it in the experimental setup, the water content of the catalyst was reduced to 1.23 w/w % by EtOH percolation ($q = 5$ cm^3/min, $t = 5$ min), and finally it was reduced to less than 1 w/w % under N_2 stream ($q = 300$ cm^3/min, $t = 5$ min).[28] A total of 20 experiments were performed by pumping OcOH and EtOH independently with two HPLC pumps (Gilson 307) at $q = 4$–6.7 cm^3/min. Reactants were mixed and preheated into a hot box at 353 K and introduced to the reactor. Molar ratio in the feed ($R_{OcOH/EtOH}$) ranged between 0.25 and 4. A series of 15 additional experiments was performed by adding DEE and EOE to the reactant mixture (0–17 and 0–33 w/w %, respectively). In this series, the previously prepared mixture was fed to the reactor with one pump ($q = 5$ cm^3/min).

Experiments were conducted in differential regime, experimentally assured for $X_{EtOH} < 14\%$ (which corresponded to $X_{OcOH} = 6\%$ at $R_{OcOH/EtOH} = 1$, $T = 463$ K), as discussed further. Reaction rates to form EOE and DEE were computed as follows

$$r_{EOE} = \frac{F_{OcOH} \cdot X_{OcOH}}{W_{cat}} S^{EOE}_{OcOH} = \frac{F_{EtOH} \cdot X_{EtOH}}{W_{cat}} S^{EOE}_{EtOH} \quad \left[\frac{mol}{h \cdot g_{cat}}\right] \tag{1}$$

$$r_{DEE} = \frac{1}{2}\frac{F_{EtOH} \cdot X_{EtOH}}{W_{cat}} S^{DEE}_{EtOH} \quad \left[\frac{mol}{h \cdot g_{cat}}\right] \tag{2}$$

W_{cat} is the dry catalyst mass, F_j the molar flow rate of alcohol species j entering the reactor, X_j the conversion of species j, and S_j^k the selectivity of reactant j toward product k at the reactor outlet defined as follows

$$S^k_j = \frac{\{\text{mole of j reacted to form k}\}}{\{\text{mole of j reacted}\}} \times 100\,[\%, \text{mol/mol}] \tag{3}$$

Some experiments were replicated to assure the reproducibility of the results. Thus, data shown have a relative experimental error lower than 3% for r_{EOE} and 6% for r_{DEE}.

Batch Reactor. A series of six experiments was carried out in a 100-cm^3 batch reactor. Setup and analysis procedure can be found elsewhere.[29] The OcOH/EtOH initial molar ratio ($R_{OcOH/EtOH}$) ranged between 0.5 and 2. The pressure was kept at 2.5 MPa with N_2 ensuring that the reaction medium was in the liquid phase. Amberlyst 70 was dried at 383 K under vacuum overnight; the water content being reduced to ≤2.25 w/w %. Then, the reactor was loaded with 70 cm^3 of OcOH/EtOH mixture, stirred, and heated up to the working temperature. When the mixture reached the desired temperature, dried resin (1–3 g) was injected into the reactor. The stirring speed was fixed at 500 rpm, ensuring enough agitation to prevent external mass-transfer effects on this reaction setup.[12] Sieved Amberlyst 70 ($d_p \leq 0.50$ mm) was used to avoid the internal mass-transfer influence on the reaction rates, as further discussed. Catalyst injection was taken as zero time. Experiments lasted 6 h and the liquid composition was analyzed hourly. Reactions rates to form DEE and to EOE were calculated by differentiating the function of the formed moles vs. time (Eq. 4)

$$r_j = \frac{1}{W_{cat}}\left(\frac{dn_j}{dt}\right) \quad \left[\frac{mol}{h \cdot g_{cat}}\right] \tag{4}$$

Results and Discussion

The same pattern was observed in the whole series of experiments. EtOH and OcOH reacted over Amberlyst 70 by forming linear ethers and water. The main ethers produced were EOE and DEE; while di-*n*-octyl ether was formed in smaller amounts. In addition to the formation of ethers, some C_8 alkenes were also formed (<2 w/w %), particularly at the highest temperatures and $R_{OcOH/EtOH}$ molar ratios of the explored range. Branched ethers and ethylene were not detected in any case.

The reaction mixture behaves nonideally, mainly due to the presence of significant amount of water.[30] Therefore, to take into account the nonideality of the alcohol-ether-water mixture, the kinetic study was made as a function of activities rather than concentrations. Activity coefficients were computed by the UNIFAC-DORTMUND predictive method.[31]

Experimental Results

Fixed-Bed Reactor Experiments. Preliminary experiments were performed at the highest temperature of the range explored (463 K) in order to check the influence of external and internal mass transfer on reaction rates of EOE and DEE formation. It was first observed that the liquid flow was drastically blocked if the catalyst was not diluted with an inert solid, as a result of the high capacity of Amberlyst 70 to swell in polar media (the volume of Amberlyst 70 in polar media is about threefold with respect to that in dry air[9]). As blank runs performed with the reactor only packed with SiC showed that it does not catalyze the reaction, Amberlyst 70 beads were diluted with SiC particles. As Figure 3A shows, a SiC/resin mass ratio of dilution (RD) $100 < RD < 150$ is suitable to avoid dilution effects. At high RD values, measured rates of DEE are highly inaccurate. Figure 3A also shows that reaction rates of EOE and DEE formation are of the same order; on the contrary, synthesis of di-*n*-octyl ether is so slow that it was difficult to measure reliable reaction rates. Finally, EtOH conversion (limiting reactant at $R_{OcOH/EtOH} = 1$) is proportional to $W/F_{EtOH,0}$, confirming that the reactor operated differentially at $X_{EtOH} \leq 14\%$ (Figure 3B).

To check the influence of external mass transfer on the measured reaction rates, a series of runs was performed by changing the superficial liquid velocity (v_s) but maintaining the ratio of dilution (RD = 100–150) and feed composition ($R_{OcOH/EtOH} = 1$). The mean particle diameter of Amberlyst 70 was $d_p = 0.20$ mm to avoid internal mass influence, as further discussed. Thus, commercial batch of Amberlyst 70 was previously crushed and sieved, as the particle diameter distribution of commercial resin ranges between $d_p = 0.40$ and 0.80 mm (Table 1). Figure 4A shows that reaction rates of EOE and DEE formation was unchanged in the whole range of v_s explored ($v_s = 0.105$–0.176 cm/s, which correspond to $q = 4$–6.7 cm^3/min) within the limits of the

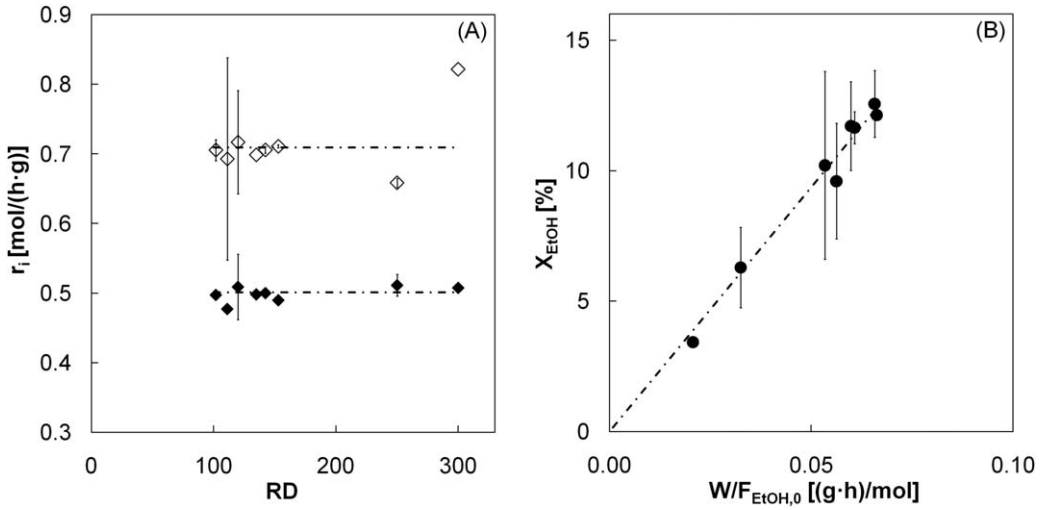

Figure 3. Effect of the RD on reaction rates of DEE (◇) and EOE (◆) formations (A). Effect of the $W/F_{EtOH,0}$ on X_{EtOH} (B).

***T* = 463 K, *P* = 2.5 MPa, *q* = 6.7 cm³/min, $R_{OcOH/EtOH} = 1$, RD = 100–150. The error bars indicate the confidence interval at a 95% probability level.**

experimental error. Hence, it is concluded that reaction rates do not depend on superficial liquid velocity over 0.105 cm/s.

The influence of internal mass transfer on reaction rates was checked by performing a series of experiments where, at the same feed composition, RD, and flow rate ($R_{OcOH/EtOH} = 1$, RD = 100–150, and $v_s = 0.176$ cm/s), catalyst samples of different particle size were used. As can be seen in Figure 4B, reaction rates of EOE and DEE formation were unchanged, within the limits of the experimental error, for $1/d_p \geq 2$ mm^{-1} (which corresponds to $d_p \leq 0.50$ mm). Commercial particle distribution of Amberlyst 70 ($d_p = 0.57 \pm 0.05$ mm, 95% confidence interval) has a mean value slightly higher than 0.50 mm, and as a result, the measured reaction rates on commercial resin samples were a bit lower than those observed free of internal mass-transfer influence.

As a consequence, measured reaction rates were free of mass-transfer resistances at $v_s \geq 0.105$ cm/s and $d_p \leq 0.50$ mm. Then, two sets of experiments were carried out to outline the influence of alcohols and ethers concentrations on the reaction rates. The experimental conditions and the obtained rates can be found in Supporting Information Table S1.

The first set of experiments was carried out by feeding OcOH and EtOH independently with a molar ratio $R_{OcOH/EtOH}$ ranging from 0.25 to 4. Figure 5 gathers the reaction rates of DEE and EOE formation obtained at the whole temperature range 423–463 K. They are plotted as a function of a_{EtOH} (5A and 5B). In this first set of experiments, it was found that $a_{OcOH} \approx 1 - a_{EtOH}$ as the activity coefficients of the two alcohols were approximately the same. As can be seen, reaction rates are highly temperature sensitive as they increase more than twice each temperature rise (≈14K). The highest EOE formation reaction rate was observed at $a_{EtOH} = a_{OcOH} \approx 0.5$ (Figure 5A) in the entire temperature range, where the driving force of the reaction of EOE synthesis, $a_{EtOH}a_{OcOH}$, has the highest value too. The presence of a rate maximum on EOE formation suggests that surface reaction is the rate-limiting step of the two reactions. As for DEE formation, the highest reaction rates were achieved in

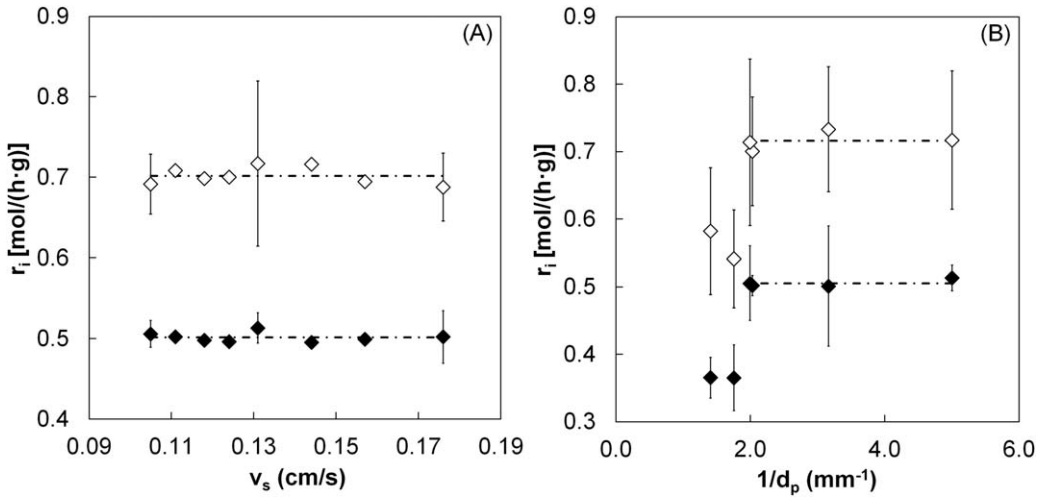

Figure 4. Effects of v_s ($d_p = 0.20$ mm) (A) and of $1/d_p$ ($v_s = 0.176$ cm/s) (B) on reaction rate of DEE (◇) and EOE (◆) formations.

***T* = 463 K, *P* = 2.5 MPa, $R_{OcOH/EtOH} = 1$, RD = 100–150. The error bars indicate the confidence interval at a 95% probability level.**

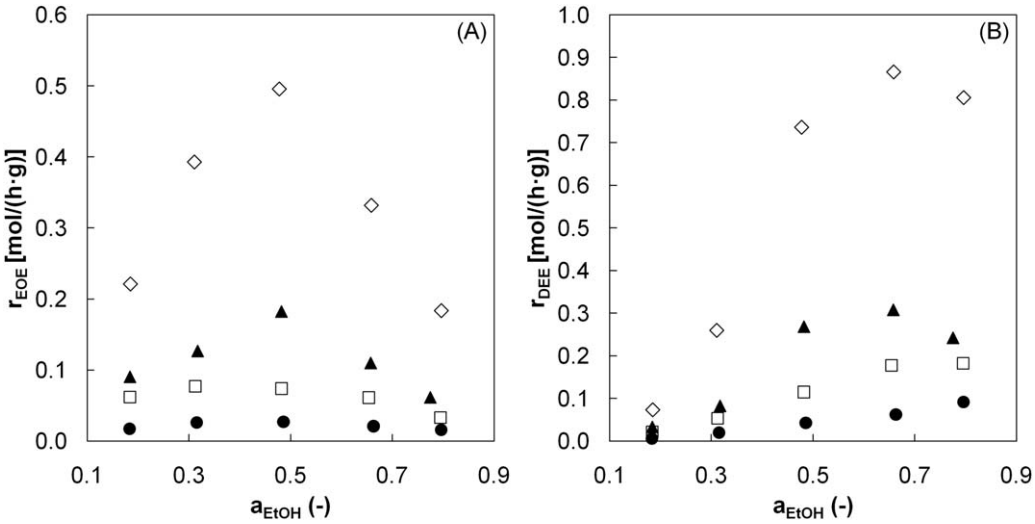

Figure 5. Reaction rates of EOE (A) and DEE (B) formation from pure reactants as a function of EtOH activity over Amberlyst 70.

●423 K, □ 437 K, ▲450 K, and ◇ 463 K.

the runs with EtOH excess, where a_{EtOH} is the highest and a_{OcOH} the lowest (Figure 5B). However, at 450 and 463 K, this maximum shifts to $a_{EtOH} \approx 0.7$. The slight shift for the DEE reaction rate maximum with temperature can be ascribed to a change in the alcohols weight in adsorption term on increasing the temperature or else to little differences in the activation energies of the two reactions.

The second set of experiments was performed by adding DEE and/or EOE to the alcohols mixture ($\leq$17 w/w % and $\leq$33 w/w %, respectively) in the feed to evaluate the effect of a_{DEE} and a_{EOE} on the reaction rate. From a kinetic standpoint, the presence of a reaction product in the feed lowers the driving force of the reaction, as a result of reactant dilution and the approach to the chemical equilibrium position. A typical procedure to stress the effect of a reaction product on the rates is by adding different quantities of such species but maintaining the other experimental conditions.[22] The effect of such species on the reaction rates can be observed graphically by plotting the reaction rates as a function of the activity of such species.

In the present work, DEE and EOE were added to the reactor feed, by varying simultaneously the molar ratio $R_{OcOH/EtOH}$ and the temperature, thus covering the whole range of concentrations and temperature explored. As a drawback of the selected procedure, the evaluation of the effect of ethers concentration on the reaction rates is less visual, as the experimental conditions are different in each experiment. It was found that reaction rates of EOE and DEE formation decreased in the presence of ethers in the feed. However, when plotting the parameter (reaction rate/driving force) as a function of ethers activity (Figure 6), it is observed that such parameter hardly changes with ethers activity despite its values are very random. As a result, the decrease in reaction rate by the presence of EOE and DEE in the reactor feed can be explained by the driving force decrease of the reaction rate to form EOE ($a_{EtOH}a_{OcOH} - a_{EOE}a_w/K_{eq,EOE}$) and to form DEE ($a_{EtOH}{}^2 - a_{DEE}a_w/K_{eq,DEE}$). Therefore, the contribution of ethers to the adsorption term of mechanistic rate models is not significant. This fact is most probably due to the EOE and DEE adsorption on acid sites is low, and therefore, they do not compete with EtOH and OcOH, what agrees with the high hydrophilicity of the resin.[6] Analogously, in the kinetic equation for the formation of DEE proposed by Kiviranta-Pääkkönen et al.,[20] it was assumed successfully that the adsorption of polar EtOH was much stronger than that of the less polar DEE. A similar behavior was observed in the effect of di-*n*-pentyl ether concentration of the reaction rate of the dehydration of 1-pentanol to ether and water on Amberlyst 70.[12]

Batch Reactor Experiments. A third set of experiments were performed to evaluate the effect of the formed water on the reaction rates at the conversion range of $0 < X_{EtOH}$ (%) < 84 and $0 < X_{OcOH}$ (%) < 65. In this setup, the reaction takes place free of diffusion influence using $d_p \leq 0.50$ mm and of external mass-transfer influence at the stirring speed of 500 rpm.[12] At the present conditions, the activity of Amberlyst 70 can be fully recovered as soon as water is removed from the reaction medium, indicating that the leaching of sulfonic groups by means of water hydrolysis is not significant.[9]

Reaction rates to form EOE and DEE decreased with the presence of reaction products in the mixture as a result of both driving forces decrease. In the fixed bed experiments, it was observed that adsorption of EOE and DEE was negligible. Nevertheless, when water was present in the reaction mixture, in significant amounts, the rate decrease cannot be explained only by the decrease of driving forces. As seen in Figure 7, the reaction rates of EOE and DEE formations were highly sensitive to the presence of water. The noticeable effect of water on the reaction rates could be explained by its competitive adsorption with EtOH and OcOH. This fact implies that the contribution of a_w to the denominator of the mechanistic models could be significant.

Modeling of kinetic data

The rate models considered in this work are based on the LHHW and ER formalisms. Taking into account the adsorption-reaction-desorption process, it is assumed that the best kinetic model for EOE formation could stem from a LHHW mechanism wherein an EtOH molecule and an OcOH molecule adsorbed on adjacent single sites react to give EOE and water. Analogously, the ER mechanism

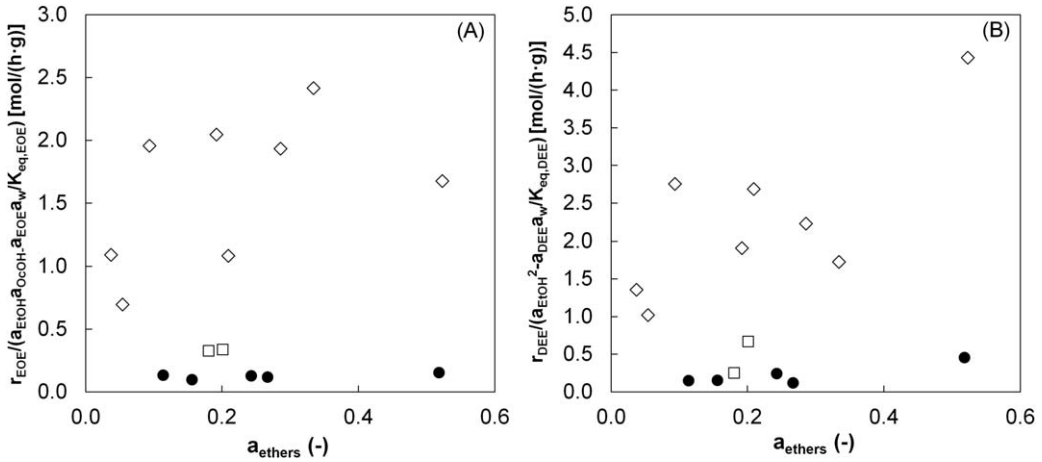

Figure 6. Reaction rates divided per the driving force of the surface reaction of EOE (A) and DEE (B) formation as a function of the a_{ethers}.

●**423 K,** □ **437 K, and** ◇ **463 K.** $P = 2.5$ **MPa.**

assumes that the EtOH molecule, or else, the OcOH molecule are not adsorbed and react from the liquid phase. Likewise, the best kinetic model of DEE formation could stem from a LHHW mechanism wherein two EtOH molecules adsorbed on adjacent single sites react to give DEE and water. The ER mechanism assumes that an EtOH molecule from the solution reacts with an EtOH molecule adsorbed on the resin. Besides, an ER mechanism implies that one of the two products is not adsorbed on the resin.

Therefore, assuming that the adsorption equilibrium of the species is reached, that EtOH, OcOH, and water adsorb competitively, and EOE and DEE adsorption is negligible unlike that of EtOH, OcOH, and water, and that surface reaction is the rate-limiting step, the basic rate models are

$$r_{EOE} = \frac{k_{EOE} \cdot \left(a_{EtOH}\, a_{OcOH} - (a_{EOE}\, a_w / K_{eq,EOE})\right)}{(1 + K_{EtOH}\, a_{EtOH} + K_{OcOH}\, a_{OcOH} + K_w a_w)^n} \quad (5)$$

$$r_{DEE} = \frac{k_{DEE} \cdot \left(a_{EtOH}^2 - (a_{DEE}\, a_w / K_{eq,DEE})\right)}{(1 + K_{EtOH}\, a_{EtOH} + K_{OcOH}\, a_{OcOH} + K_w a_w)^n} \quad (6)$$

Three parts can be distinguished in rate expressions (Eqs. 5 and 6): the kinetic term, the driving force, and the adsorption term.

- The kinetic terms, k_{EOE} and k_{DEE}, are a combination of the rate coefficient for surface reaction and adsorption equilibrium constants. The particular form how such parameters are grouped depends on the considered mechanism (LHHW or ER).
- The driving force accounts for how far is the equilibrium position. This term decreases with the equilibrium approach due to the inverse reactions, EOE and DEE hydrolysis. The values of the thermodynamic equilibrium constants for the two reactions, $K_{eq,i}$, were obtained from the chemical composition at equilibrium and are reported elsewhere.[30]
- The adsorption term accounts for the adsorption of each species on the active sites of the catalysts. Simplified models can be obtained by assuming the adsorption of some species to be negligible with respect to the others. Likewise, the number of simplified models are doubled if the fraction of unoccupied sites in the catalyst is considered significant or not (by taking values of 0 if the number of unoccupied sites is assumed to be negligible, or 1 if this assumption is neglected). Besides the adsorption contribution of each species, another parameter to be determined is the exponent of the adsorption

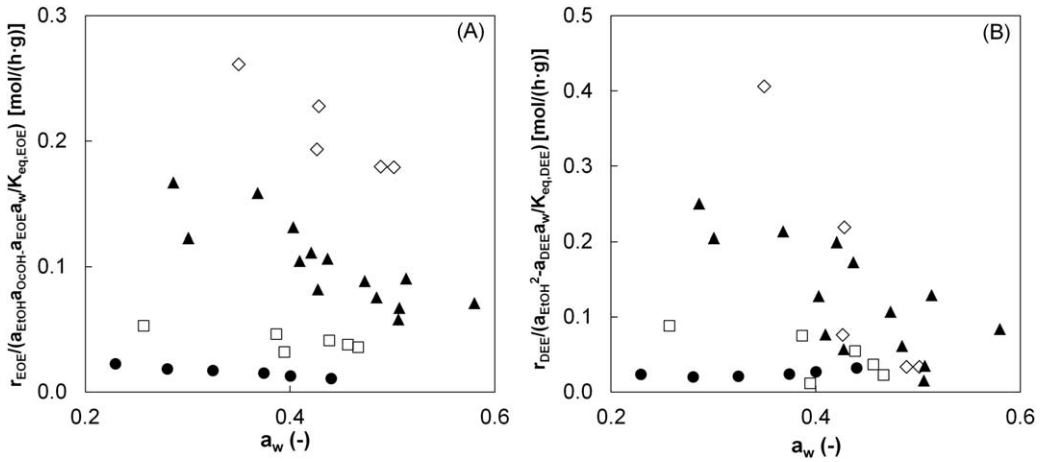

Figure 7. Reaction rates divided per the driving force of the surface reaction of EOE (A) and DEE (B) formation as a function of the a_w.

●**423 K,** □ **437 K,** ▲**450 K, and** ◇ **463 K.** $P = 2.5$ **MPa.**

Table 2. Kinetic Models Tested with n Values Ranging from 1 to 3

Model	r_{EOE}	r_{DEE}
1	$\frac{k_{EOE}\left(a_{EtOH}a_{OcOH}-a_{EOE}a_w/K_{eq,EOE}\right)}{\left(a_{EtOH}+(K_w/K_{EtOH})a_w\right)^n}$	$\frac{k_{DEE}\left(a_{EtOH}^2-a_{DEE}a_w/K_{eq,DEE}\right)}{\left(a_{EtOH}+(K_w/K_{EtOH})a_w\right)^n}$
2	$\frac{k_{EOE}\left(a_{EtOH}a_{OcOH}-a_{EOE}a_w/K_{eq,EOE}\right)}{\left(a_{OcOH}+(K_w/K_{EtOH})a_w\right)^n}$	$\frac{k_{DEE}\left(a_{EtOH}^2-a_{DEE}a_w/K_{eq,DEE}\right)}{\left(a_{OcOH}+(K_w/K_{EtOH})a_w\right)^n}$
3	$\frac{k_{EOE}\left(a_{EtOH}a_{OcOH}-a_{EOE}a_w/K_{eq,EOE}\right)}{\left(a_{EtOH}+(K_{OcOH}/K_{EtOH})a_{OcOH}+(K_w/K_{EtOH})a_w\right)^n}$	$\frac{k_{DEE}\left(a_{EtOH}^2-a_{DEE}a_w/K_{eq,DEE}\right)}{\left(a_{EtOH}+(K_{OcOH}/K_{EtOH})a_{OcOH}+(K_w/K_{EtOH})a_w\right)^n}$
4	$\frac{k_{EOE}\left(a_{EtOH}a_{OcOH}-a_{EOE}a_w/K_{eq,EOE}\right)}{\left(1+K_{EtOH}a_{EtOH}+K_wa_w\right)^n}$	$\frac{k_{DEE}\left(a_{EtOH}^2-a_{DEE}a_w/K_{eq,DEE}\right)}{\left(1+K_{EtOH}a_{EtOH}+K_wa_w\right)^n}$
5	$\frac{k_{EOE}\left(a_{EtOH}a_{OcOH}-a_{EOE}a_w/K_{eq,EOE}\right)}{\left(1+K_{OcOH}a_{OcOH}+K_wa_w\right)^n}$	$\frac{k_{DEE}\left(a_{EtOH}^2-a_{DEE}a_w/K_{eq,DEE}\right)}{\left(1+K_{OcOH}a_{OcOH}+K_wa_w\right)^n}$
6	$\frac{k_{EOE}\left(a_{EtOH}a_{OcOH}-a_{EOE}a_w/K_{eq,EOE}\right)}{\left(1+K_{EtOH}a_{EtOH}+K_{OcOH}a_{OcOH}+K_wa_w\right)^n}$	$\frac{k_{DEE}\left(a_{EtOH}^2-a_{DEE}a_w/K_{eq,DEE}\right)}{\left(1+K_{EtOH}a_{EtOH}+K_{OcOH}a_{OcOH}+K_wa_w\right)^n}$

term related to the number of active sites that participates in the rate-limiting step (n). It is quoted in the literature that in the case of ion-exchange resins an active site can be considered as a cluster of sulfonic groups rather than an individual one.[32] In this work, the exponent of the adsorption term has been varied from 1 to 3. As further discussed, no more additional sites were needed to describe the experimental data.

Table 2 shows all the rate models for EOE and DEE formation (36 equations), derived from Eqs. 5 and 6, fitted to the experimental data. Optimal values of the parameters have been obtained by minimization of the sum of squared relative errors (SSRR; Eq. 7). Relative errors were used instead of the absolute ones as the relative error is assumed to be of the same order in the whole temperature range

$$\mathrm{SSRR}=\sum\left(\frac{r_{exp}-r_{calc}}{r_{exp}}\right)^2 \tag{7}$$

Figure 8 gathers the goodness of the fit for the different rate models. A value of 1 corresponds to the minimum of SSRR, and as a result, to the best mathematical fit. Therefore, Model 3 with $n=1$ is the best mathematical model to explain the experimental reaction rates of EOE and DEE formations. It should be noted that Models 5 were rejected because they presented negative adsorption equilibrium constants. A closer look at that model leads to infer for both reactions:

a. The best model is explained by the participation of 1 active site (or cluster) in the surface-reaction step, which corresponds to ER formalism.
b. The number of unoccupied sites in the catalyst during the reaction is not significant, what seems reliable in liquid-phase reactions catalyzed by solids.
c. The best kinetic model of EOE and DEE formations is that where adsorption of both EtOH and OcOH is present. This fact is in agreement with the literature that states that both OcOH and EtOH are adsorbed on the acidic ion-exchange resins, possibly in a similar composition to the bulk solution.[6]

The best model of EOE formation (Model 3 with $n=1$; Table 2) is consistent with two plausible reaction mechanisms. OcOH from solution (R_2OH) reacts with EtOH adsorbed on one active site (R_1OH) to give the water adsorbed on the resin and EOE released instantaneously to liquid phase, or conversely, EtOH from solution (R_2OH) reacts with OcOH adsorbed on an active site (R_1OH).

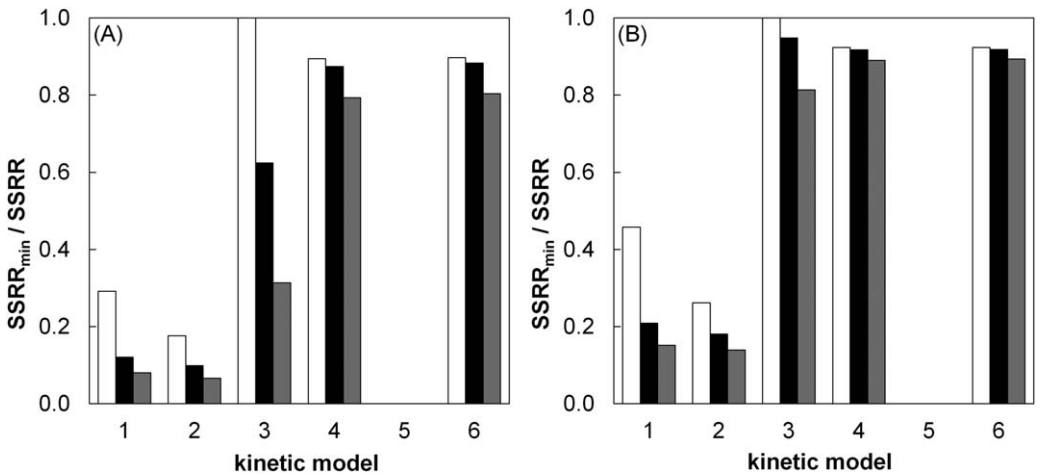

Figure 8. Comparison of goodness of fit in terms of $SSRR_{min}/SSRR$ of EOE (A) and DEE (B) formations.

□ $n=1$, ■ $n=2$, and ■ $n=3$.

Table 3. Apparent Activation Energies and Adsorption Quotients Obtained from the Proposed Models (Eqs. 8 and 9)

Parameter	EOE	DEE
E_a (kJ/mol)	105 ± 4	100 ± 5
K_w/K_{EtOH}	11.7 ± 1.0	11.7 ± 1.0
K_{OcOH}/K_{EtOH}	0.5 ± 0.1	0.5 ± 0.1

$$R_1OH + \sigma \rightleftharpoons R_1OH \cdot \sigma$$

$$R_1OH \cdot \sigma + R_2OH \rightleftharpoons EOE + W \cdot \sigma$$

$$W \cdot \sigma \rightleftharpoons W + \sigma$$

The best model for DEE formation (Model 3 with $n = 1$; Table 2) coincides with the one proposed by Kiviranta-Pääkkönen et al.[20] EtOH from solution reacts with EtOH adsorbed on an active site giving place to water adsorbed on the resin surface and DEE released instantaneously to liquid phase.

$$EtOH + \sigma \rightleftharpoons EtOH \cdot \sigma$$

$$EtOH \cdot \sigma + EtOH \rightleftharpoons DEE + W \cdot \sigma$$

$$W \cdot \sigma \rightleftharpoons W + \sigma$$

Accordingly, the best rate models for the two reactions are

$$r_{EOE}\left[\frac{mol}{h \cdot g}\right] = \frac{7.04\times10^{11}\exp(-12,620/T)\left(a_{EtOH}\,a_{OcOH} - a_{EOE}\,a_{water}/K_{eq,EOE}\right)}{a_{EtOH} + 0.5a_{OcOH} + 11.7a_{water}}; \quad K_{eq,EOE} = \exp\left(\frac{3374.8}{T} - 4.3\right) \tag{8}$$

$$r_{DEE}\left[\frac{mol}{h \cdot g}\right] = \frac{2.10\times10^{11}\exp(-11,983/T)\left(a_{EtOH}^2 - a_{DEE}\,a_{water}/K_{eq,DEE}\right)}{a_{EtOH} + 0.5a_{OcOH} + 11.7a_{water}}; \quad K_{eq,DEE} = \exp\left(\frac{1691}{T} - 1.4\right) \tag{9}$$

Uncertainty of the fitted parameters is shown in Table 3. As it is observed, both kinetic terms have Arrhenius-type dependence on temperature. On the contrary, no significant dependence of the K_{OcOH}/K_{EtOH} and K_w/K_{EtOH} ratios on the temperature was found, within the temperature range explored. This fact indicates that the experimental data were not sensitive enough to determine the differences between the adsorption enthalpies of OcOH and water with respect to that of EtOH. Consequently, both equilibrium adsorption quotients were regarded as constants within the temperature range 423–463 K.

In Figure 9, the reaction rates of EOE formation estimated by Eq. 8 (Figure 9A) and of DEE by Eq. 9 (Figure 9B) are compared to the experimental ones. As observed, both rate models are able to represent well rate data, regardless of the used setup. Besides, the residuals show random distribution in the whole range of measured reaction rates (Figure 10). In addition, it is to be noted that the proposed rate models are able to predict accurately rate data regardless the presence of ethers in the reaction mixture. Accordingly, this supports the assumption that EOE and DEE do not compete with alcohols to be adsorbed on the resin.

Apparent activation energy values ($E_{a,i}$) were obtained from the kinetic term of the rate models (Eqs. 8 and 9). Figure 11 illustrates the Arrhenius-type dependence of the apparent rate constants (11A and 11B, respectively). Similar values of apparent activation energy for EOE formation, $E_{a,EOE} = 105 \pm 4$ kJ/mol, than for DEE formation, $E_{a,DEE} = 100 \pm 5$ kJ/mol, were obtained. It is to be noted that the obtained E_a value for EOE formation from OcOH and EtOH on Amberlyst 70 is slightly lower than that obtained on a preliminary study over Dowex 50Wx2 (117 ± 5 kJ/mol) and in the range of the dehydration reactions of 1-pentanol to di-*n*-pentyl ether and 1-hexanol to di-*n*-hexyl ether (115 ± 5 and 108 ± 5 kJ/mol, respectively) on the same catalyst Amberlyst 70.[6] As for DEE formation, the

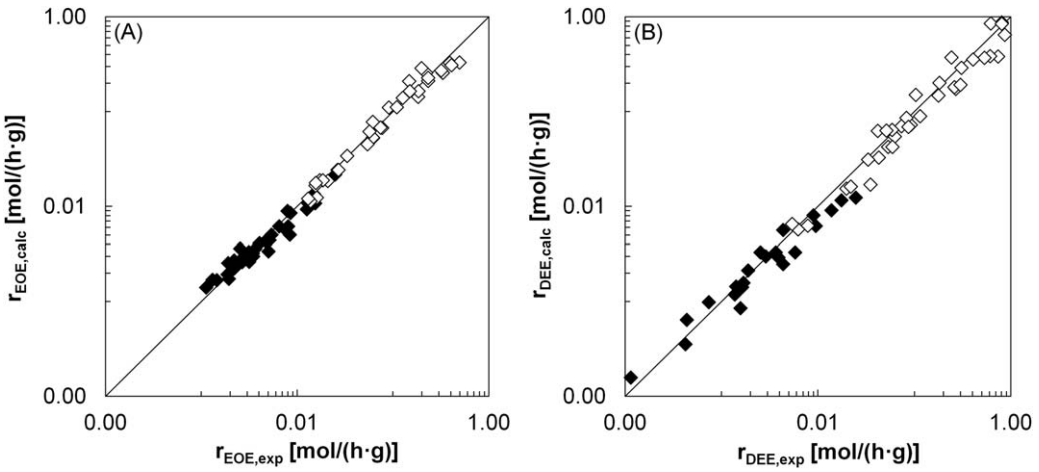

Figure 9. Reaction rates estimated by Eq. 8 (A) and Eq. 9 (B) vs. experimental ones.

Open symbols represent data obtained in the fixed-bed reactor and closed symbols those obtained in the batch reactor.

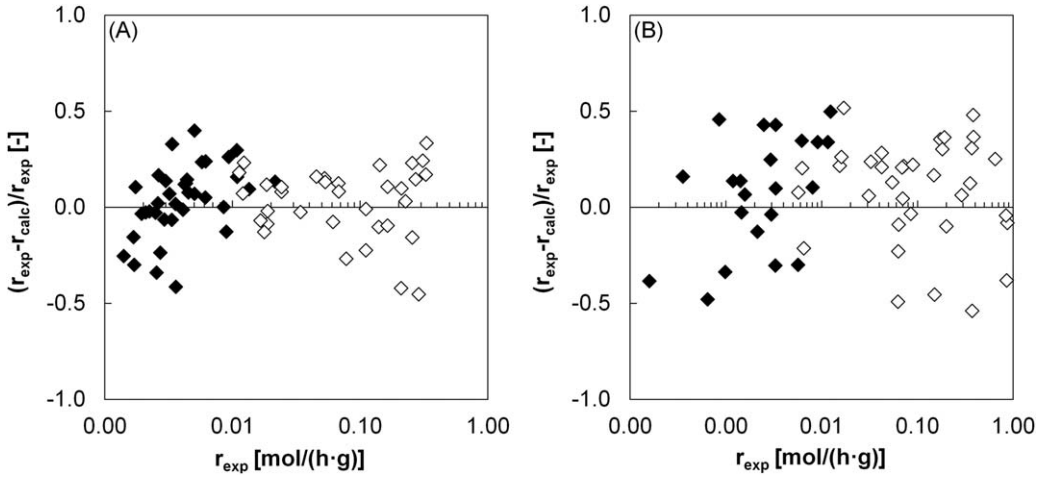

Figure 10. Residuals distribution for Eq. 8 (A) and Eq. 9 (B).

Open symbols represent data obtained in the fixed-bed reactor and closed symbols those obtained in the batch reactor.

obtained E_a value (100 ± 5 kJ/mol) is in agreement with the value reported by Kiviranta-Pääkkönen et al.[20] (89.9 ± 18.8 kJ/mol) within the limits of the experimental error (95% probability level).

As for the quotients of adsorption equilibrium constants, $K_w/K_{EtOH} = 11.7 \pm 1.0$ and $K_{OcOH}/K_{EtOH} = 0.5 \pm 0.1$ values were obtained. Thus, it is inferred that $K_w >> K_{EtOH} > K_{OcOH}$. This trend is in agreement with the polarity of the compounds and the high water affinity of the resin. The role ascribed to water in Eqs. 8 and 9 assumes a strong competitive adsorption with EtOH and OcOH for acid sites, being K_w 12-fold K_{EtOH} and 23-fold K_{OcOH}. Therefore, reaction rates to EOE and to DEE are greatly affected by the presence of water in the liquid phase.

However, the strong inhibitor effect of water on EOE formation on an acid resin are much lower than that reported on the synthesis of bisphenol A, being water adsorption equilibrium constant values two orders of magnitude higher than those of acetone and phenol.[33] This fact is most probably a result of the higher polarity of alcohols with respect to acetone and phenol. Thus, EtOH and OcOH compete more efficiently with water for adsorption on the resin. In the case of the etherification of isoamylenes with ethanol, the inhibitory effect of water on the dehydration of EtOH to form DEE is negligible as it is promptly consumed giving place to 2-methyl-2-butanol (tert-amyl alcohol).[20]

Conclusions

The reaction between 1-octanol and ethanol to give EOE is performed in the liquid phase at 413–463 K on Amberlyst 70. EOE formation takes place in parallel with the dehydration reactions of ethanol and 1-octanol to DEE and di-*n*-octyl ether, respectively. The dehydration reaction of ethanol to DEE is the main side one in the temperature and concentration ranges explored showing reaction rates comparable to those of EOE formation, whereas reaction rate of di-*n*-octyl ether formation is very low. As a consequence, a kinetic study of the reactions of EOE and DEE formation has been carried out. Rate data were obtained using a fixed bed reactor working in a differential regime, and in a batch reactor wherein high conversions of ethanol (up to 84 %) and 1-octanol (up to 65 %) were achieved.

Because reaction medium is nonideal, mechanistic rate models in terms of compound activities are proposed to describe both the formation of EOE and of DEE. Reaction rate equation for EOE synthesis derives from an ER mechanism in which an EtOH molecule adsorbed on the resin

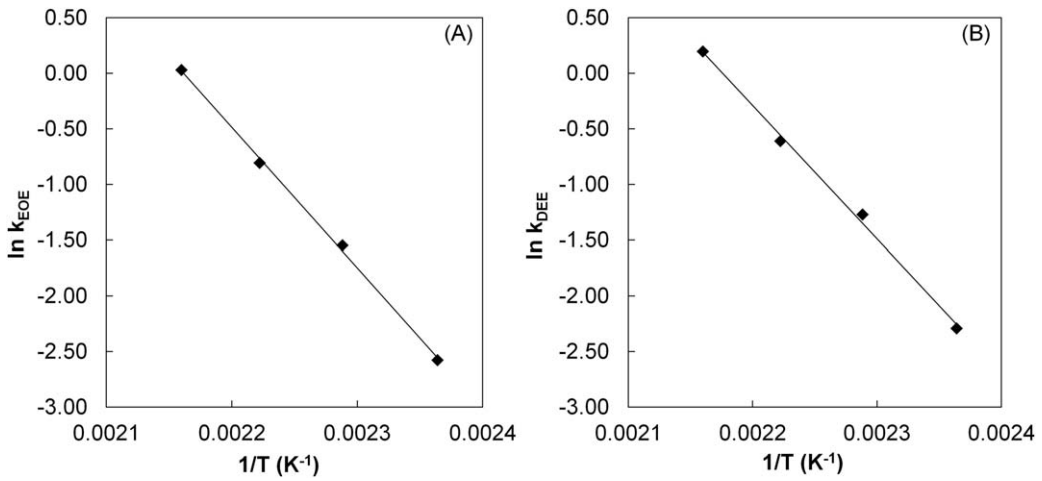

Figure 11. Arrhenius plots of kinetic term of EOE (A) and of DEE (B) formation reactions.

reacts with an OcOH molecule, or vice versa (as the true mechanism is indistinguishable from only kinetic information). DEE formation would take part by the reaction of an EtOH molecule adsorbed onto the resin with a second one from the liquid phase. In both cases, it is assumed that surface reaction is the rate-limiting step.

The two reaction models have the same adsorption term, in agreement with a scenario of competitive adsorption between reactants and reaction products. It has found that the fraction of free actives sites is negligible compared to those occupied by ethanol, 1-octanol, and water. In addition, adsorption of EOE and DEE are nonsignificant in front of those of alcohols and water. Thus, it can be assumed that EOE and DEE are released directly to the liquid phase, whereas reaction rates were highly sensitive to the water presence, clearly showing a strong inhibitory effect. Eventually, the apparent activation energy for EOE synthesis is about 105 ± 4 kJ/mol, a similar dependence on temperature to that of DEE formation, 100 ± 5 kJ/mol.

Acknowledgments

Financial support was provided by the State Education, Universities, Research & Development Office of Spain (project CTQ2010-16047). The authors thank Rohm and Haas for supplying ion exchange resin Amberlyst 70.

Notation

σ = active center
a_j = activity of compound j
DEE = diethyl ether
d_p = mean particle diameter, mm
$E_{a,i}$ = apparent activation energy of reaction i, kJ/mol
EOE = ethyl octyl ether
EtOH = ethanol
F_j = molar flow rate of compound j, mol/h
k = kinetic term, mol/h/g
K_j = adsorption equilibrium constant of compound j
$K_{eq,i}$ = thermodynamic equilibrium constant of reaction i
n = number of active sites that take part in the rate-limiting step
n_j = moles of compound j
OcOH = 1-octanol
q = volume flow rate, cm^3/min
r_j = reaction rate of formation of compound j, mol/h/g
$R_{OcOH/EtOH}$ = initial OcOH/EtOH molar ratio
RD = SiC/resin mass ratio of dilution
S_j^k = selectivity of reactant j towards product k, mol/mol %
SSRR = sum of squared relative residuals
t = time
T = temperature
X_j = conversion of compound j
V_{sp} = specific volume of the swollen polymer phase, m^3/kg
v_s = superficial flow velocity, cm/s
W_{cat} = dry catalyst mass, g

Literature Cited

1. Pecci GC, Clerici MG, Giavazzi F, Ancillotti F, Marchiona M, Patrini R. Oxygenated diesel fuels-structure and properties correlation. In: ECOFUEL (AgipPetroli Sector), editors. IX International Symposium on Alcohol Fuels. ISAF – Firenze '91: Proceedings of the IX International Symposium on Alcohol Fuels; Florence, Italy. Milan: ECOFUEL (AgipPetroli Sector), November 12–15, 1991: 321–335.
2. Olah GA, inventor; Olah GA, assignee. Cleaner burning and cetane enhancing diesel fuel supplements. US Patent US5520710A. May 28, 1996.
3. Eberhard J, inventor; MAN Nutzfahrzeuge AG, assignee. Diesel fuel based on ethanol. US Patent Application 20100242347. September 30, 2010.
4. Bringué R, Ramírez E, Iborra M, Tejero J, Cunill F. Influence of acid ion-exchange resins morphology in a swollen state on the synthesis of ethyl octyl ether from ethanol and 1-octanol. *J Catal*. 2013; 304:7–21.
5. Casas C, Guilera J, Ramírez E, Iborra M, Tejero J. Reliability of the synthesis of C_{10}–C_{16} linear ethers from 1-alkanols over acidic ion exchange resins. *Biomass Convers Bioref*. 2013;3:27–37.
6. Guilera J, Bringué R, Ramírez E, Iborra M, Tejero J. Comparison between ethanol and diethyl carbonate as ethylating agents for ethyl octyl ether synthesis over acidic ion-exchange resins. *Ind Eng Chem Res*. 2012;51:16525–16530.
7. Siril PF, Cross HE, Brown DR. New polystyrene sulfonic acid resin catalysts with enhanced acidic and catalytic properties. *J Mol Catal A*. 2008;279:63–68.
8. Alonso DM, Bond JQ, Serrano-Ruiz JC, Dumesic JA. Production of liquid hydrocarbon transportation fuels by oligomerization of biomass-derived C_9 alkenes. *Green Chem*. 2010;12:992–999.
9. Guilera J, Ramírez E, Fité C, Iborra M, Tejero J. Thermal stability and water effect on ion-exchange resins in ethyl octyl ether production at high temperature. *Appl Catal A*. 2013;467:301–309.
10. The Dow Chemical Company. Available at: http://www.dow.com. Accessed on April 2, 2014.
11. Purolite Corporation. Available at: http://www.purolite.com. Accessed on April 2, 2014.
12. Bringué R, Iborra M, Tejero J, Izquierdo JF, Cunill F, Fité C, Cruz VJ. Thermally stable ion-exchange resins as catalysts for the liquid-phase dehydration of 1-pentanol to di-n-pentyl ether (DNPE). *J Catal*. 2006;244:33–42.
13. Chandak HS, Lad NP, Upare PP. Recyclable Amberlyst-70 as a catalyst for Biginelli reaction: an efficient one-pot green protocol for the synthesis of 3,4-dihydropyrimidin-2(1H)-ones. *Catal Lett*. 2009;131: 469–473.
14. Bond JQ, Alonso DM, Wang D, West RM, Dumesic JA. Integrated catalytic conversion of γ-valerolactone to liquid alkenes for transportation fuels. *Science*. 2010;5969:1110–114.
15. Li X, Gunawan R, Lievens C, Wang Y, Mourant D, Wang S, Wu H, Garcia-Perez M, Li C. Simultaneous catalytic esterification of carboxylic acids and acetalisationof aldehydes in a fast pyrolysis bio-oil from mallee biomass. *Fuel*. 2011;90:2530–2537.
16. Alonso DM, Bond JQ, Wang D, Dumesic JA. Activation of Amberlyst-70 for alkene oligomerization in hydrophobic media. *Top Catal*. 2011;54:447–457.
17. Orjuela A, Yanez AJ, Santhanakrishnan A, Lira CT, Miller DJ. Kinetics of mixed succinic acid/acetic acid esterification with Amberlyst 70 ion exchange resin as catalyst. *Chem Eng J*. 2012;188: 98–107.
18. Gates BC, Johanson LN. Langmuir-Hinshelwood kinetics of the dehydration of methanol catalyzed by cation exchange resin. *AIChE J*. 1971;17:981–983.
19. Gates BC, Johanson LN. The dehydration of methanol and ethanol catalyzed by polystyrene sulfonate resins. *J Catal*. 1969;14: 69–76.
20. Kiviranta-Pääkkönen PK, Struckmann LK, Linnekoski JA, Krause AOI. Dehydration of the alcohol in the etherification of isoamylenes with methanol and ethanol. *Ind Eng Chem Res*. 1998;37: 18–24.
21. Collin JR, Ramprasad D, inventors; Rohm And Haas Company, assignee. Methods, systems and catalysts for the hydration of olefins. European Patent 1479665 A1. November 24, 2004.
22. Hosseininejad S, Afacan A, Hayes RE. Catalytic and kinetic study of methanol dehydration to dimethyl ether. *Chem Eng Res Des*. 2012;90:825–833.
23. Kabel RL, Johanson LN. Reaction kinetics and adsorption equilibria in the vapor-phase dehydration of ethanol. *AIChE J*. 1962;8:621–628.
24. Mollavali M, Yaripour F, Atashi H, Sahebdelfar S. Intrinsic kinetics study of dimethyl ether synthesis on (-Al_2O_3). *Ind Eng Chem Res*. 2008;47:3265–3273.
25. Lu W, Teng L, Xiao W. Simulation and experimental study of dimethyl ether synthesis from syngas in a fluidized bed reactor. *Chem Eng Sci*. 2004;59:5455–5464.
26. Silva VMTM, Rodrigues AE. Synthesis of diethylacetal: thermodynamic and kinetic studies. *Chem Eng Sci*. 2001;56:1255–1263.
27. Silva VMTM, Rodrigues AE. Novel process for diethylacetal synthesis. *AIChE J*. 2005;51:2752–2768.

28. Iborra M, Tejero J, Cunill F, Izquierdo JF, Fité C. Drying of acidic macroporous styrene-divinylbenzene resins with 12–20 cross-linking degree. *Ind Eng Chem Res*. 2000;39:1416–1422.
29. Guilera J, Bringué R, Ramírez E, Iborra M, Tejero J. Synthesis of ethyl octyl ether from diethyl carbonate and 1-octanol over solid catalysts. A screening study. *Appl Catal A*. 2012;413–414:21–29.
30. Guilera J, Ramírez E, Iborra M, Tejero J, Cunill F. Experimental study of chemical equilibria in the liquid-phase reaction between 1-octanol and ethanol to 1-ethoxyoctane. *J Chem Eng Data*. 2013; 58:2076–2082.
31. Witting R, Lohmann J, Gmehling J. Vapor-liquid equilibria by UNIFAC group contribution. 6. Revision and extension. *Ind Eng Chem Res*. 2003;42:183–188.
32. Buttersack C, Widdecke J, Klein J. The concept of variable active centres in acid catalysis: part I. Alkylation of benzene with olefins catalyzed by ion-exchange resins. *J Mol Catal*. 1986;38:365–381.
33. Jerabek K, Odnoha J, Setinek K. Kinetics of the synthesis of bisphenol A. *Appl Catal*. 1988;36:129–138.

Manuscript received Feb. 5, 2014, and revision received Apr. 30, 2014.